Journal for ImmunoTherapy of Cancer

Dual roles of IRE1α inhibition in reversing mitochondrial ROS-induced CD8$^+$ T-cell senescence and exerting direct antitumor effects in multiple myeloma

Yike Wan ,[1] Jingjing Wang,[2] Mengping Chen,[1] Junying Wang,[1] Fajun Nan,[3] Honghui Huang,[1] Zhiqiang Liu,[2] Jian Hou[1]

To cite: Wan Y, Wang J, Chen M, *et al*. Dual roles of IRE1α inhibition in reversing mitochondrial ROS-induced CD8$^+$ T-cell senescence and exerting direct antitumor effects in multiple myeloma. *Journal for ImmunoTherapy of Cancer* 2025;**13**:e011044. doi:10.1136/jitc-2024-011044

► Additional supplemental material is published online only. To view, please visit the journal online (https://doi.org/10.1136/jitc-2024-011044).

YW and JW contributed equally.

Accepted 08 May 2025

For numbered affiliations see end of article.

Correspondence to
Professor Jian Hou;
houjian@medmail.com.cn

Professor Zhiqiang Liu;
zqliu@sdfmu.edu.cn

ABSTRACT

Background Multiple myeloma (MM) is characterized by the proliferation of malignant plasma cells within the bone marrow (BM) microenvironment, which significantly contributes to immune suppression of CD8$^+$ T cells. Our previous research identified that dysregulation of the IRE1α-XBP1s-SLC38A2 axis leads to decreased glutamine uptake and senescence of CD8$^+$ T cells in MM. However, the underlying mechanisms of T-cell senescence remain unclear.

Methods Single-cell RNA sequencing was used to analyze mitochondrial function in CD8$^+$ T cells in MM. The effects of XBP1s and SLC38A2 on mitochondrial reactive oxygen species (mtROS) were evaluated by flow cytometry under loss-of-function experiments. An IRE1α inhibitor (17#) was administered to explore its effects on T-cell senescence and MM cell growth. RNA sequencing was employed to disclose pathway alterations in T cells treated with 17#. The Vk*MYC mouse model was used to assess the impact of 17# on CD8$^+$ T cell senescence and anti-myeloma effects.

Results BM-derived CD8$^+$ T cells from patients with MM exhibited downregulated expressions of genes critical for glutamine transport (SLC38A2), mitochondrial respiratory chain, and ATP synthesis, while genes associated with ROS were upregulated. Suppression of XBP1s in CD8$^+$ T cells resulted in decreased mtROS levels, whereas inhibition of SLC38A2 increased mtROS levels. Compound 17# significantly reduced senescence marker KLRG1 expression and increased perforin expression in nutrient-deprived BM CD8$^+$ T cells from healthy donors and in BM CD8$^+$ T cells from patients with MM, while promoting T-cell proliferation. Importantly, 17# did not impair the viability of peripheral blood mononuclear cells from healthy donors or alter the immune phenotypes of healthy CD8$^+$ T cells. The NPR2-cGMP-PKG pathway was activated by IRE1α inhibition in restoring T-cell function. Furthermore, 17# exhibited direct inhibitory effects on MM cells. In Vk*MYC mouse model, 17# decreased mtROS levels in BM CD8$^+$ T cells, reduced the proportion of senescent (KLRG1$^+$CD57$^+$CD28$^-$) T cells, and resulted in a lower tumor burden.

Conclusion Inhibiting IRE1α represents a promising strategy to reverse the senescence of CD8$^+$ T cells by mitigating mtROS production. This dual mechanism not only rejuvenates T cells but also directly targets myeloma cells, offering a novel therapeutic approach for MM treatment.

WHAT IS ALREADY KNOWN ON THIS TOPIC

⇒ Multiple myeloma (MM) is characterized by the proliferation of malignant plasma cells within the bone marrow (BM) microenvironment, leading to immune suppression of CD8$^+$ T cells.
⇒ The IRE1α-XBP1s pathway is critical for the survival and proliferation of MM cells and has been identified as a therapeutic target.
⇒ Our previous research has shown that dysregulation of the IRE1α-XBP1s-SLC38A2 axis results in decreased glutamine uptake and senescence of CD8$^+$ T cells in MM.

WHAT THIS STUDY ADDS

⇒ This study demonstrates that inhibiting IRE1α reduces mitochondrial reactive oxygen species levels in BM CD8$^+$ T cells in MM, thereby reversing T-cell senescence and enhancing their anti-myeloma efficacy.
⇒ IRE1α inhibition not only rejuvenates CD8$^+$ T cells but also directly inhibits the growth of MM cells, offering a dual mechanism of action.
⇒ The study identifies the NPR2-cGMP-PKG pathway as a critical mediator in restoring CD8$^+$ T-cell function through IRE1α inhibition.

HOW THIS STUDY MIGHT AFFECT RESEARCH, PRACTICE OR POLICY

⇒ These findings suggest that targeting IRE1α could be a promising therapeutic strategy for MM, potentially improving the efficacy of immunotherapy by reversing CD8$^+$ T-cell senescence.
⇒ The dual action of IRE1α inhibitors on both CD8$^+$ T cells and MM cells could lead to the development of more effective combination therapies.
⇒ Future research and clinical trials may focus on the application of IRE1α inhibitors in MM and other cancers characterized by immune suppression and endoplasmic reticulum stress.

BACKGROUND

Multiple myeloma (MM) is characterized by the clonal proliferation and survival of neoplastic plasma cells within the bone marrow microenvironment (BME).[1] The BME facilitates the growth and therapeutic resistance of MM cells. A critical pathogenic mechanism contributing to MM cells is the suppression of $CD8^+$ T cells.[2–4] Our previous research,[5] employing single-cell RNA sequencing (scRNA-seq) and in vitro experiments, has revealed an upregulation of the IRE1α-XBP1s pathway within the unfolded protein response (UPR) in $CD8^+$ T cells obtained from the bone marrow (BM) of patients with MM, with a corresponding increase in the expression of the transcription spliced XBP1s, which plays a role in cellular metabolism regulation.

IRE1α, an endoplasmic reticulum (ER) stress sensor, activates its endoribonuclease activity on sensing stress, leading to the splicing of XBP1 mRNA (XBP1s). XBP1s translocates to the nucleus and binds to ER stress response elements, thereby initiating the transcription and translation of UPR target genes.[6] The IRE1α-XBP1s pathway is critical for the survival and proliferation of MM cells, establishing it as a validated therapeutic target.[7] Preclinical studies have demonstrated the anti-myeloma effects of IRE1α inhibitors, including in human MM xenograft models.[8 9] However, most of these studies have been conducted in immunodeficient mice, primarily focusing on the direct effects of IRE1α inhibitors on MM cells, with limited investigation into their impacts on T-cell function.

Our previous findings demonstrated that XBP1s directly suppress the expression of the glutamine transporter gene SLC38A2, resulting in reduced intracellular glutamine levels.[5] This dysregulation of glutamine metabolism is particularly critical for T cells, as their fate and functionality are intimately linked to metabolic pathways.[10] SLC38A2 encodes the sodium-coupled neutral amino acid transporter 2 (SNAT2), which is essential for glutamine uptake in T cells, thereby playing a pivotal role in maintaining T-cell function and viability.[11] The importance of glutamine in cellular processes, especially in T-cell survival and activation, underscores the need to understand the regulatory mechanisms governing its transport and utilization.[12] Given the established link between the IRE1α-XBP1s pathway and glutamine transport in T cells, it is plausible that IRE1α inhibitors could modulate T-cell function by reprogramming glutamine metabolism. However, the precise mechanisms by which IRE1α inhibitors exert these effects on T cells remain to be elucidated.

Moreover, we have previously identified that $CD8^+$ T cells in patients with MM predominantly manifest a senescent phenotype rather than an exhausted state, characterized by the heightened expression of KLRG1 and CD57, coupled with a lack of CD28 expression.[5] Only a subset of these cells exhibits features of exhaustion, as indicated by the presence of LAG3 and TIGIT. Interference with the XBP1s-SLC38A2 axis in T cells can regulate the expression of senescence-related indicators. While the mechanisms underlying $CD8^+$ T-cell senescence induced by this signaling pathway warrant further investigation, mitochondrial dysfunction is recognized as one of the key metabolic factors contributing to cellular senescence. An imbalance in mitochondrial dynamics leads to the accumulation of mitochondrial reactive oxygen species (mtROS), depletion of ATP, and damage to mitochondrial DNA, ultimately resulting in senescence.[13]

This study aims to investigate the regulatory role of targeting the XBP1s-SLC38A2 axis on $CD8^+$ T-cell senescence, employing both in vivo and in vitro experiments. Our findings reveal that inhibiting IRE1α leads to a reduction in mtROS levels within $CD8^+$ T cells, thereby enhancing anti-myeloma immunity by reversing cellular senescence. A deeper understanding of the metabolic regulation mechanisms in $CD8^+$ T cells will contribute to the advancement of immune therapeutic strategies in MM.

METHODS

Subjects, samples and chemicals

For scRNA-seq, BM and peripheral blood (PB) samples were obtained from 10 patients with newly diagnosed MM according to the criteria of the International Myeloma Working Group[14] and from three healthy individuals matched to the patients in terms of age and sex. Then mononuclear cells were extracted and used for subsequent sequencing. Samples of patients with MM were collected on initial diagnosis and after two cycles of therapy involving bortezomib, cyclophosphamide, and dexamethasone. All patients were hospitalized between March 2019 and July 2020 in the department of hematology at Ren Ji Hospital. For in vitro studies, BM and PB samples were acquired from an additional 10 patients with newly diagnosed MM and 10 age/sex-matched healthy donors. MM cell lines including U266, H929, RPMI 8226, MM1S, and acute lymphoblastic leukemia cell line (Molt4) were used for experiments of drug treatment, cell transfection and RNA sequencing. 17# is a small molecule compound that abrogates the UPR in cancer cells subjected to diverse ER stress stimuli.[15] 17# was first screened from the NCDS library and then synthesized by Professor Fajun Nan (The National Center for Drug Screening, Shanghai, China).

Single-cell RNA sequencing

scRNA-seq was performed by Novogene (Beijing, China) with 10x Genomics platform. Demultiplexed reads were mapped to the genome using the CellRanger pipeline (10x Genomics) and default parameters. The specific methods have been described previously.[5 16]

RNA sequencing

IRE1α inhibitor-treated or untreated Molt4 cells were sequenced on an Illumina NovaSeq 6000 platform with a paired-end 150 cycles run, generating approximately 50 million reads per sample. The sequencing was

performed at LC-Bio Technologies (Hangzhou, China), following their standard operating procedures.

Gene functional enrichment analysis

Differentially-expressed genes (DEGs) of T-cell clusters were identified using Seurat based on profiles of gene expressions. Differential expressions between samples were analyzed using the edgeR package in R V.3.6.2 to obtain zone-specific marker genes. To predict potential functions of T-cell clusters, the enrichment of genes in Gene Ontology (GO) terms and Kyoto Encyclopedia of Genes and Genomes (KEGG) pathways was analyzed based on the clusterProfiler package in R, with correction for gene length bias. Enrichment in GO terms was considered significant if it was associated with corrected $p<0.05$. Heatmaps showing GO and KEGG enrichment in different T-cell clusters were generated using k-means clustering analysis of DEGs in the pheatmap package in R. Gene Sets Enrichment Analysis (GSEA) was conducted using clusterProfiler V.3.12.0 in R. The Molecular Signatures Database[17] was used to collect gene sets and molecular signatures for annotation. Gene set permutations were performed to obtain normalized enrichment scores, with a cut-off p value of 0.05 to filter significant enrichments.

Lymphocyte separation and T-cell culture

BM and PB samples were obtained under an Institutional Review Board-approved protocol. Mononuclear cells were isolated by density gradient with Ficoll-Paque (GE HealthCare, USA), and then were stimulated using 25 µL/mL anti-CD3/CD28 antibodies (STEMCELL Technologies, Canada) with 300 IU/mL IL-2 (PeproTech, USA) for 3 days. $CD8^+$ T cells were isolated using a magnetic negative selection kit (Miltenyi Biotec, Germany) and cultured in T-cell culture medium (STEMCELL Technologies, Canada). The stimulation and activation methods of purified $CD8^+$ T cells from BM of patients with MM or healthy donors are the same as those of mononuclear cells.

Lentivirus transfection

For silencing XBP1s, sequence encoding short hairpin (sh) RNA targeting the XBP1 gene was inserted into the PGMLV-HU6-MCS-CMV-ZsGreen1-PGK-Puro plasmid (Genomeditech). For silencing SLC38A2, the sequence encoding shRNA targeting the SLC38A2 gene was inserted into the CMV-cop GFP-T2a-puro-H1-MCS plasmid (ZORIN Biological Technology). The lentiviral vector PGMLV-CMV-MCS-EF1-mScarlet-T2A-Blasticidin (Genomeditech) containing XBP1s complementary DNA (cDNA) was used for overexpression experiments. Control plasmid was prepared using scrambled shRNA sequences. Sequences and primers are shown in online supplemental table 1. The vectors were co-transfected into 293T cells with packaging plasmids (TIANGEN), and recombinant lentivirus in the culture medium was harvested. $CD8^+$ T cells and Molt4 cells were transduced with lentivirus and cultured at 5×10^5 cells/mL for 4 days.

Flow cytometry analysis

For surface marker staining, about 2×10^5 T cells or MM cells were re-suspended in phosphate-buffered saline containing 2% fetal bovine serum and stained with the antibody cocktail for 30 min at room temperature in the dark. For intracellular cytokine staining, cells were stained for intracellular cytokines after fixation and permeabilization followed by cell surface marker staining. All samples were acquired with a DxFLEX system (Beckman Coulter) and analyzed using FlowJo software (V.10.5.3). Antibodies used for cell surface staining or intracellular staining were listed in online supplemental table 2.

MitoSOX Red-based flow cytometry for detecting mtROS

About 2×10^5 T cells or MM cells were incubated with 5 µM MitoSOX Red (MedChemExpress, China) for 20 min at 37°C, protected from light. After gently washing the cells three times with warm buffer to remove excess MitoSOX Red, the mean fluorescence intensity was measured to detect mitochondrial superoxide.

Quantitative RT-PCR

Total RNA was isolated from 5×10^6 Molt4 cells, $CD8^+$ T cells, MM cells or Vk*MYC mice BM cells and reverse-transcribed into cDNA using HiScript III All-in-one RT SuperMix (Vazyme). The cDNA was subjected to quantitative real-time polymerase chain reaction (qRT-PCR) using the primers listed in online supplemental table 3 under the following conditions: 94°C for 4 min, followed by 40 cycles of 94°C for 1 min, 56°C for 1 min, and 72°C for 1 min. Expression of marker genes was normalized against that of GAPDH using the $2^{\Delta\Delta CT}$ method.

Cell viability with CCK8

Suspensions of $CD8^+$ T cells, peripheral blood mononuclear cells (PBMCs), Molt4 cells or MM cells were inoculated (100 µL/well) in a 96-well plate. IRE1α inhibitor, dimethyl sulfoxide (DMSO), and blank culture medium were added separately. Cells were incubated for an appropriate length of time (24, 48 or 72 hours) in the incubator. CCK-8 solution (10 µL) was added to each well of the plate and the plate was incubated for 3 hours. The absorbance at 450 nm was measured using a microplate reader.

In vivo experiments

C57BL/6J mice (6–8 weeks of age, both sexes, caged mice) received intravenous injection of murine myeloma Vk*MYC cells (1×10^6 cells per mouse) and 3 weeks later, Vk*MYC mice received intraperitoneal injection (i.p.) of 17# (20 mg/kg) (n=5) or vehicle (n=5), respectively, to investigate the impact of 17# on T cells and MM cells in vivo. 17# was dissolved in 2.5% DMSO+2.5% Kolliphor+95% methyl cellulose (0.5 g/100 mL). After 14 days of treatment, spleen and BM were collected for subsequent experiments. The mice were euthanized by severing their spinal cords. The proportions of plasma cells and T cells in BM and spleen samples, as well as T-cell immunophenotypes, were detected by flow cytometry.

The expression of Xbp1s in BM cells was detected by qRT-PCR.

Before treatment, only mice in good health were included; those with obvious diseases or abnormal behavior were excluded. The mice were randomly divided into two groups before the treatment to ensure that each group was comparable at baseline. All experimental procedures, including treatment administration, sample collection, and measurements, were standardized and performed according to a predefined protocol. In both groups, one mouse died due to infection before harvest. We used the ARRIVE checklist when writing our report.[18]

The Vk*MYC cell line, derived from MYC-driven genetically engineered mice, exhibits plasma cell malignancy with features mimicking human MM, including monoclonal paraprotein secretion, osteolytic lesions, and progressive splenic tumor growth.[19] This model retains an immunocompetent microenvironment, enabling investigation of T cell-myeloma interactions. Importantly, Vk*MYC tumors are responsive to immunomodulatory agents, making them suitable for evaluating therapies targeting both myeloma cells and immune senescence.

Statistical analysis

Sequences were analyzed using R, plots were generated using ggplot2. P values were calculated using GraphPad Prism (GraphPad Software, California, USA). Variables following a normal distribution, as verified by the Shapiro-Wilk test, were analyzed using Student's t-test. Variables not following normal distribution were analyzed using the Mann-Whitney test. Gene expression differences in sequencing were analyzed using the Wilcoxon rank-sum test. P value<0.05 was considered statistically significant.

RESULTS

Glutamine transport and mitochondrial function pathways are downregulated in CD8$^+$ T cells of patients with MM

In our previous study, we collected BM and PB samples from 10 patients with newly diagnosed MM and three age-matched healthy controls, isolated mononuclear cells for scRNA-seq, and discovered that cytotoxic T cells mainly displayed features of senescence.[5] To further explore the mechanisms of CD8$^+$ T-cell senescence in BME, we analyzed the scRNA-seq data and subclustered cytotoxic T cells from BM into nine cell types (figure 1A). We next performed GSEA analysis and identified glutamine transport, mitochondrial and ATP synthesis-related pathways that were negatively enriched in BM CD8$^+$ T cells from patients with newly diagnosed MM (figure 1B and C). Similar results of downregulation of mitochondrial function-related pathways were also found in CD8$^+$ T cells in PB of patients with MM (online supplemental figure 1A).

The downregulation of enzymes integral to the electron transport chain, which is responsible for generating the majority of ATP through oxidative phosphorylation, indicates a compromised energy production capacity in both BM and PB CD8$^+$ T cells from patients with MM (figure 1D, online supplemental table 4 and supplemental figure 1B). Moreover, the expression of mitochondrial transcription factor A (TFAM), a crucial regulator of mitochondrial maintenance and organization of the mitochondrial genome, was markedly lower in BM and PB CD8$^+$ T cells from patients with MM compared with healthy controls (figure 1E and online supplemental figure 1C). Collectively, these data indicated a positive correlation between impaired metabolic processes and the senescence of CD8$^+$ T cells in patients with MM.

Targeting the XBP1s-SLC38A2 axis in CD8$^+$ T cells modulates mtROS levels

Our initial study has shown that the XBP1s-SLC38A2 axis in CD8$^+$ T cells of patients with MM leads to a decrease in intracellular glutamine content and cell senescence.[5] Therefore, the connection between metabolic processes and senescence is worth further exploration. Compared with healthy controls, the ROS synthesis regulatory pathway was enriched in BM and PB CD8$^+$ T cells from patients with MM (figure 2A, online supplemental table 4 and supplemental figure 1D). To evaluate whether the XBP1s-SLC38A2 axis in CD8$^+$ T cells affects the level of mtROS, which is a significant cause of cell senescence, we generated SLC38A2 and XBP1s individually knockdown cells. The production of mtROS was increased when SLC38A2 deficiency in healthy BM CD8$^+$ T cells under the condition of complete medium (figure 2B and C). Meanwhile, healthy BM CD8$^+$ T cells were cultured in a glucose-free medium to simulate the stress environment, and inhibition of XBP1 expression resulted in reduced mtROS levels (figure 2B and C). Consistent results were also observed in the T lymphocyte cell line Molt4 cells (figure 2D and E). Taken together, these data prove the involvement of the XBP1s-SLC38A2 axis in the regulation of mtROS levels within T cells.

IRE1α inhibition attenuates senescence and augments cytotoxicity of CD8$^+$ T cells

Given that IRE1α inhibitors inhibited the XBP1s-SLC38A2 axis by interfering with the splicing of XBP1, we further investigated the effect of an IRE1α inhibitor (17#) on T-cell senescence. Our previous scRNA-seq data indicated that the senescence-related marker that was significantly elevated in BM and PB CD8$^+$ T cells of patients with MM was KLRG1 (online supplemental figure 2A). Flow cytometry was performed on PB samples from additional patients with newly diagnosed MM and healthy controls to validate the high expression of senescence surface markers KLRG1 on CD8$^+$ effector memory T/effector T (Tem/Teff) cells in patients with MM (online supplemental figure 2B). Notably, the expression of exhaustion markers was higher in patients with MM's PB CD8$^+$ Tem/Teff cells than in normal controls, but the proportion was lower than that of senescence markers. To create an in vitro model of T-cell senescence, we used a glucose-deficient medium to create a stressful cell

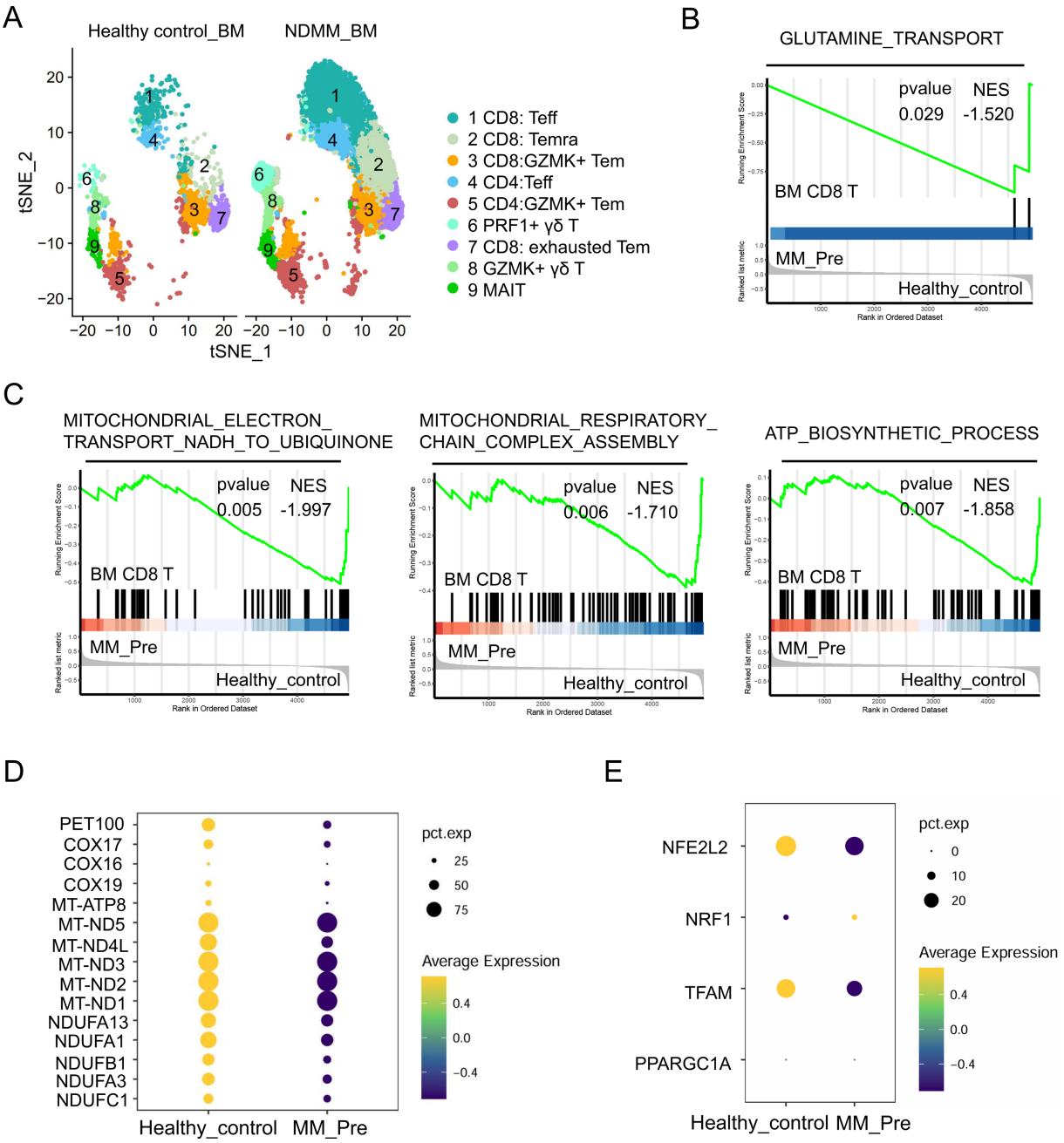

Figure 1 Glutamine transport and mitochondrial function pathways are downregulated in BM-derived CD8$^+$ T cells of patients with MM. (A) Stratification and cell-type identification of cytotoxic T cells in BM samples from three healthy controls and 10 patients with newly diagnosed MM before treatment. Clusters were distinguished by different colors. (B) GSEA enrichment plots for glutamine transport in CD8$^+$ T cell clusters from BM samples in patients with pretreatment MM compared with healthy controls. (C) GSEA enrichment plots for mitochondria-associated pathways in CD8$^+$ T cell clusters from BM samples in patients with pretreatment MM compared with healthy controls. (D) Dot plots showing average expressions of mitochondria-associated markers in CD8$^+$ T-cell clusters from BM samples in patients with pretreatment MM compared with healthy controls. (E) Dot plots showing average expressions of TFAM pathway markers in CD8$^+$ T-cell clusters from BM samples in patients with pretreatment MM compared with healthy controls. BM, bone marrow; GSEA, Gene Sets Enrichment Analysis; MM, multiple myeloma; NES, normalized enrichment score; TFAM, mitochondrial transcription factor A; tSNE, t-distributed stochastic neighbor embedding.

culture environment. Glucose deprivation significantly upregulated both the expression of senescence marker (KLRG1) and exhaustion marker (LAG3) and XBP1s mRNA levels in Molt4 cells (online supplemental figure 2C). In contrast, 17# significantly suppressed XBP1s mRNA expression (online supplemental figure 2D) and increased cell proliferation (online supplemental figure 2E). In addition, 17# treatment reduced the expression of KLRG1 while only affecting LAG3 at high concentration (online supplemental figure 2F and G), increased the production of CD107a and interferon (IFN)-γ (online supplemental figure 2G).

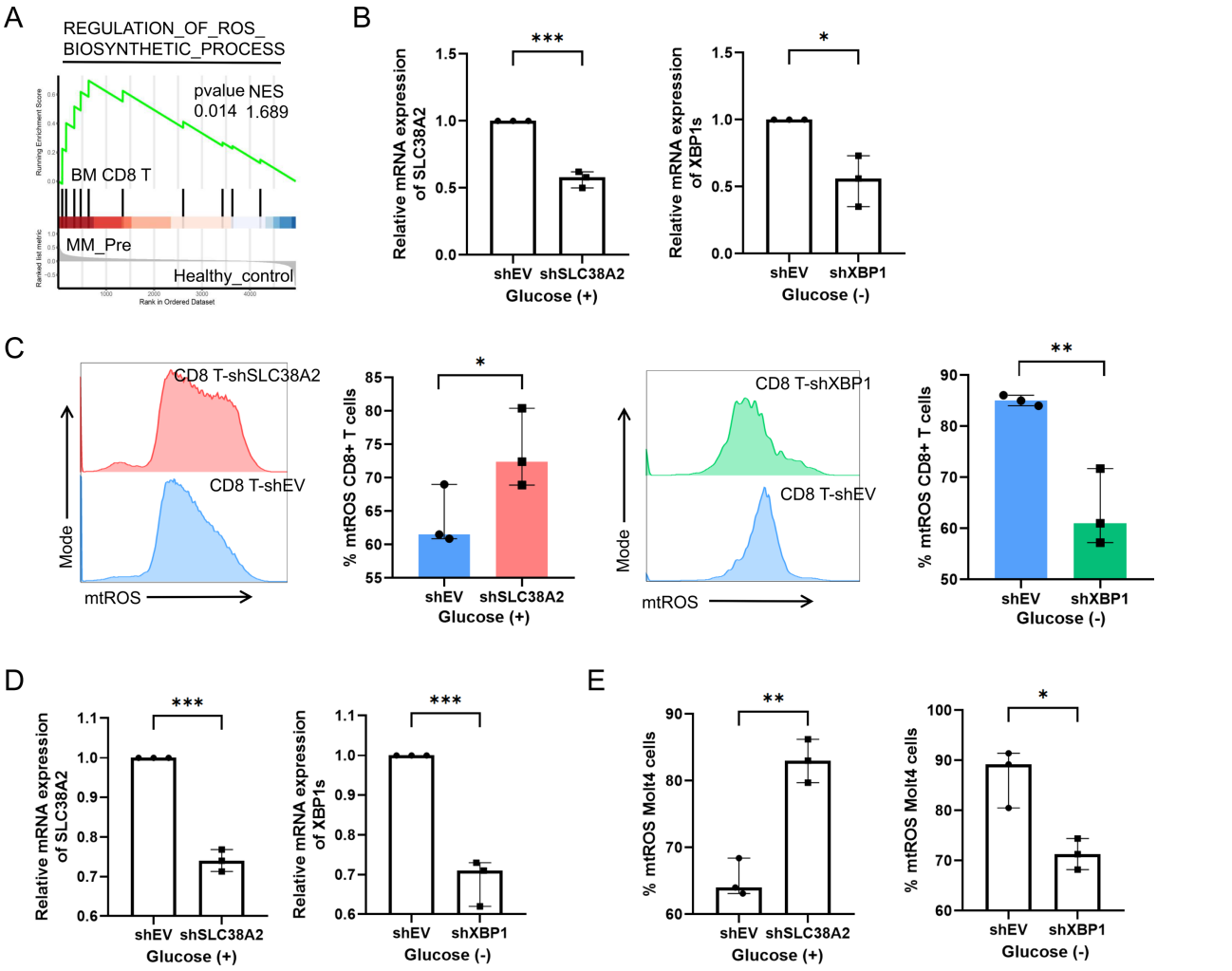

Figure 2 Targeting the XBP1s-SLC38A2 axis in CD8$^+$ T cells modulates mtROS levels. (A) Gene Sets Enrichment Analysis enrichment plots for regulation of ROS biosynthetic process in CD8$^+$ T-cell clusters from BM samples in patients with pretreatment MM compared with healthy controls. (B) Mononuclear cells from BM of healthy donors were activated in complete medium supplemented with anti-CD3/CD28 antibodies and interleukin-2 for 3 days. Subsequently, CD8$^+$ T cells were isolated using magnetic cell sorting and then were lentiviral transfected with shRNA against SLC38A2, XBP1 or empty vector (EV). After 4 days, CD8$^+$ T cells transfected with shRNA against SLC38A2 or EV were cultured for 3 days in complete medium, while CD8$^+$ T cells transfected with shRNA against XBP1 or EV were cultured for 3 days in glucose-free medium. Relative mRNA expressions of SLC38A2 and XBP1s in CD8$^+$ T cells were detected by qRT-PCR. Data are presented as mean values±SD (n=3). Two-sided unpaired t-test, $^*p<0.05$, $^{***}p<0.001$. (C) Percentages of mtROS expressing CD8$^+$ T cells from (B) were detected by flow cytometry. Data are presented as median with interquartile range (n=3 biologically independent experiments). Two-sided unpaired t-test, $^*p<0.05$, $^{**}p<0.01$. (D) Molt4 cells were transfected with shRNA against SLC38A2, XBP1 or EV. After 4 days, Molt4 cells transfected with shRNA against SLC38A2 or EV were cultured for 3 days in complete medium, while Molt4 cells transfected with shRNA against XBP1 or EV were cultured for 3 days in glucose-free medium. Relative mRNA expressions of SLC38A2 and XBP1s in Molt4 cells were detected by qRT-PCR. Data are presented as mean values±SD (n=3). Two-sided unpaired t-test, $^{***}p<0.001$. (E) Percentages of mtROS expressing Molt4 cells from (D) were detected by flow cytometry. Data are presented as median with IQR (n=3). Two-sided unpaired t-test, $^*p<0.05$, $^{**}p<0.01$. BM, bone marrow; MM, multiple myeloma; mRNA, messenger RNA; mtROS, mitochondrial reactive oxygen species; NES, normalized enrichment score; qRT-PCR, quantitative real-time polymerase chain reaction; sh, short hairpin.

To verify the role of 17# in primary CD8$^+$ T cells, we isolated mononuclear cells from BM of healthy donors, activated them in complete medium containing anti-CD3/CD28 antibodies and interleukin (IL)-2 for 3 days, and then positively selected CD8$^+$ T cells using magnetic beads. These CD8$^+$ T cells were next cultured in glucose-free or glucose-containing medium with different concentrations of 17# or DMSO for 48 hours. The results showed that glucose deprivation significantly increased the expressions of KLRG1, CD57, LAG3 and TIGIT, and decreased perforin expression in BM-derived CD8$^+$ T cells (figure 3A and online supplemental figure 3A). Treatment with 17# reduced KLRG1 expression, increased perforin expression, and promoted the proliferation of CD8$^+$ T cells in response to glucose deprivation (figure 3A, B), with no significant effect on other exhaustion (LAG3,

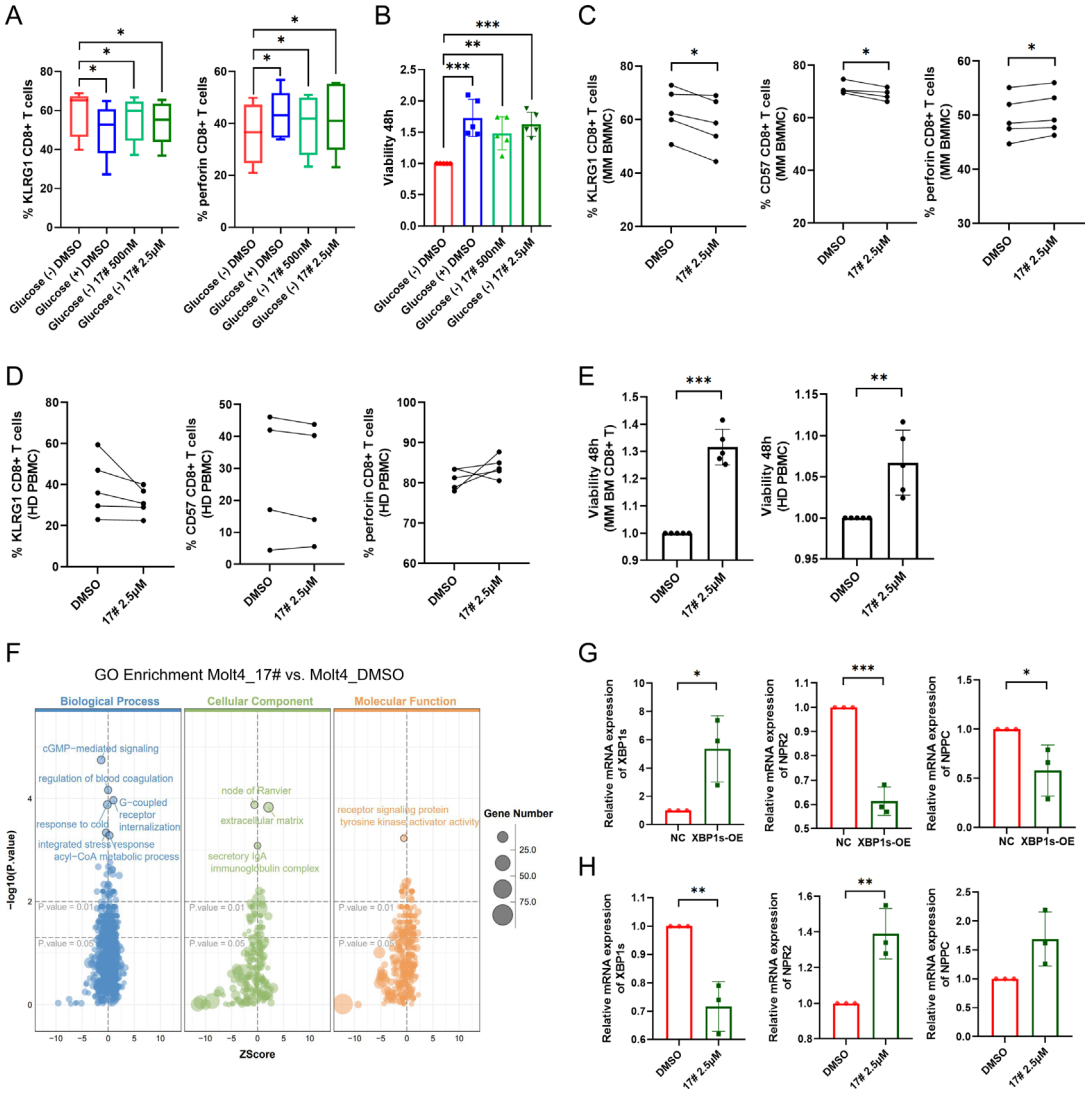

Figure 3 IRE1α inhibition attenuates senescence and activates NPR2-cGMP-PKG in CD8$^+$ T cells. (A) Mononuclear cells from BM of healthy donors were activated in complete medium supplemented with anti-CD3/CD28 antibodies and IL-2 for 3 days. Subsequently, CD8$^+$ T cells were isolated using magnetic cell sorting and then were cultured for 48 hours in either glucose-free or glucose-containing media, with varying concentrations of 17# or DMSO. Percentages of KLRG1 and perforin-expressing CD8$^+$ T cells were assessed by flow cytometry. Data are presented as mean values±SD (n=5). Two-sided paired t-test, *p<0.05. (B) Viability of CD8$^+$ T cells in (A) was assessed by CCK8. Data are presented as mean values±SD (n=5). Two-sided unpaired t-test, **p<0.01, ***p<0.001. (C) CD8$^+$ T cells were isolated from mononuclear cells from BM of five patients with newly diagnosed MM using magnetic bead sorting, and then were cultured for 48 hours in glucose-free medium supplemented with either 17# or DMSO, along with anti-CD3/CD28 antibodies and IL-2. Percentages of KLRG1, CD57 and perforin-expressing CD8$^+$ T cells were assessed by flow cytometry. Data are presented as mean values±SD (KLRG1 and perforin n=5; CD57 n=4). Two-sided paired t-test, *p<0.05. (D) PBMCs were obtained from five healthy donors (HD), and then were cultured for 48 hours in complete medium supplemented with either 17# or DMSO, along with anti-CD3/CD28 antibodies and IL-2. Percentages of KLRG1, CD57 and perforin-expressing CD8$^+$ T cells were assessed by flow cytometry. Data are presented as mean values±SD (KLRG1 and perforin n=5; CD57 n=4). Two-sided paired t-test. (E) Viability of CD8$^+$ T cells in (C) and PBMCs in (D) were assessed by CCK8. Data are presented as mean values±SD (n=5). Two-sided unpaired t-test, **p<0.01, ***p<0.001. (F) Molt4 cells were treated with 17# (5 μM) or DMSO for 48 hours in medium without glucose. Bubble plots showing the top enriched terms by GO pathway analysis for upregulated pathways in 17# treated Molt4 cells compared with the DMSO group. (G) BM CD8$^+$ T cells of healthy donors were lentivirally transfected with XBP1s overexpressing vector (OE) or empty vector (NC). Relative mRNA expressions of XBP1s, NPR2 and NPPC in BM CD8$^+$ T cells were detected by qRT-PCR. Data are presented as mean values±SD (n=3). Two-sided unpaired t-test, *p<0.05, ***p<0.001. (H) Mononuclear cells from BM of healthy donors were activated in complete medium supplemented with anti-CD3/CD28 antibodies and IL-2 for 3 days. Subsequently, CD8$^+$ T cells were isolated using magnetic cell sorting and then were cultured for 48 hours in glucose-free media, treated with 17# or DMSO. Relative mRNA expressions of XBP1s, NPR2 and NPPC in BM CD8$^+$ T cells were detected by qRT-PCR. Data are presented as mean values±SD (n=3). Two-sided unpaired t-test, **p<0.01. BM, bone marrow; DMSO, dimethyl sulfoxide; GO, Gene Ontology; IL, interleukin; MM, multiple myeloma; mRNA, messenger RNA; PBMC, peripheral blood mononuclear cell; qRT-PCR, quantitative real-time polymerase chain reaction.

PD-1, TIGIT, and TIM3) and activation (CD25 and CD69) markers (online supplemental figure 3A).

To investigate the impact of 17# on $CD8^+$ T cells in patients with MM, we obtained mononuclear cells from BM of five patients with newly diagnosed MM. $CD8^+$ T cells were subsequently isolated using magnetic bead sorting and cultured for 48 hours in glucose-free medium supplemented with either 17# or DMSO, along with anti-CD3/CD28 antibodies and IL-2. Our results demonstrated that treatment with 17# significantly reduced KLRG1, CD57, and LAG3 expressions while enhancing perforin expression in $CD8^+$ T cells derived from BM of patients with MM (figure 3C and online supplemental figure 3B). To evaluate the potential off-target effects of 17#, we treated PBMCs from healthy donors, cultured in complete medium, with 17# or DMSO. The results indicated that 17# did not significantly affect the expressions of KLRG1, CD57, perforin, or exhaustion and activation markers in these cells (figure 3D and online supplemental figure 3C). We found that 17# promoted the proliferation of $CD8^+$ T cells derived from MM BM and normal PBMCs, although the proliferative response in the latter was less pronounced (figure 3E). This difference may be attributed to varying degrees of ER stress experienced by these cells.

Furthermore, we examined the impact of 17# on $CD4^+$ T cells. Compound 17# increased the proportion of $CD4^+$ Tem/Teff cells in the BM of patients with newly diagnosed MM, and reduced the proportion of $CD4^+$ naive T (Tn) cells (online supplemental figure 3D). It had no significant effect on the $CD4^+$ T-cell subpopulation in healthy PBMCs (online supplemental figure 3D). Compound 17# also reduced the expressions of KLRG1, CD57 and LAG3 in $CD4^+$ Tem/Teff cells in the BM of patients with newly diagnosed MM (online supplemental figure 3E), but had no significant effect on the expressions of senescence, exhaustion and activation markers in $CD4^+$ Tem/Teff cells in healthy PBMCs (online supplemental figure 3E).

IRE1α inhibition activates NPR2-cGMP-PKG signaling pathway in $CD8^+$ T cells

To gain insight into the underlying mechanisms on 17#, we performed RNA-seq in Molt4 cells treated with 17# (5 µM) or DMSO for 48 hours in medium without glucose. The results exhibited different biological processes, cellular components, and molecular functions (figure 3F). By profiling the transcriptome data, we noticed that the cGMP-PKG signaling pathway (enriched from expressions of NPR2 and NPPC) and metabolic pathway in Molt4 cells were significantly upregulated after 17# treatment in GO and KEGG analysis (figure 3F and online supplemental figure 4). The cGMP-PKG pathway has been demonstrated to regulate mitochondrial dynamics, like fusion and fission events, which are of great significance for maintaining mitochondrial integrity and function.[20]

To directly investigate whether XBP1s regulates the cGMP-PKG pathway in $CD8^+$ T cells, we conducted in vitro overexpression experiments using healthy human BM $CD8^+$ T cells. Overexpression of XBP1s via lentiviral transduction significantly suppressed mRNA levels of NPR2 and NPPC, which are critical regulators of the cGMP-PKG pathway (figure 3G). Conversely, treatment with 17# in BM $CD8^+$ T cells derived from patients with MM restored NPR2 expression (figure 3H), consistent with our RNA-seq data indicating activation of the cGMP-PKG pathway. These findings establish a direct regulatory relationship between XBP1s and NPR2, suggesting that inhibition of IRE1α alleviates XBP1s-mediated repression of NPR2, thereby activating cGMP-PKG signaling.

IRE1α inhibition suppresses the proliferation of MM cells independently of the XBP1s-SLC38A2 axis

IRE1α inhibitors have been shown to perturb the proliferation of MM cells, we further studied whether they may modulate the expression of SNAT2 through the XBP1s-SLC38A2 axis, which potentially impacts glutamine uptake and leads to a worse nutrient-deprived tumor microenvironment. We treated four kinds of MM cell lines (U266, H929, RPMI 8226, and MM1S) with 17# and found that the proliferation of all MM cell lines was inhibited after 72 hours (figure 4A), and the expression level of XBP1s mRNA was significantly downregulated (figure 4B). Compound 17# had no significant effect on SNAT2 in MM cells, and the positive proportion of SNAT2 expressing MM cells remained consistently low (figure 4C). There are various glutamine transporters, with different cells predominantly expressing distinct types. Based on our prior single-cell sequencing results in patients with MM and healthy donors, in comparison to healthy controls, malignant plasma cells exhibit significantly higher expression of SLC1A5, SLC7A5, and SLC38A5, rather than SLC38A2 (SNAT2).[5] In order to investigate whether 17# has any influence on these highly expressed transporters, we treated MM cells with 17# and found that 17# did not significantly alter the mRNA levels of SLC1A5, SLC7A5 and SLC38A5 (figure 4D). Collectively, these results indicate that IRE1α inhibition does not promote the expression of SLC38A2 through the XBP1s-SLC38A2 axis in MM cells, nor does it affect the expressions of the major glutamine transporters.

IRE1α inhibition reverses $CD8^+$ T-cell senescence and reduces tumor burden in Vk*MYC myeloma mouse model

To investigate the impact of IRE1α inhibitor on antitumor immune responses, we used the Vk*MYC myeloma mouse model. After being treated with 17# for 14 days, we isolated cells from spleen and BM (figure 5A). Splenic phenotyping showed that 17# reduced the tumor burden induced by MM cells (figure 5B). Consistent with this observation, the proportion of BM $B220^-CD138^+$ plasma cells in the 17# group declined compared with the vehicle group (figure 5C). Moreover, 17# led to a decrease in the mRNA expression of XBP1s in BM cells (figure 5D), as well as the level of mtROS in BM $CD8^+$ T cells (figure 5E). Flow cytometry analysis indicated that the proportion of

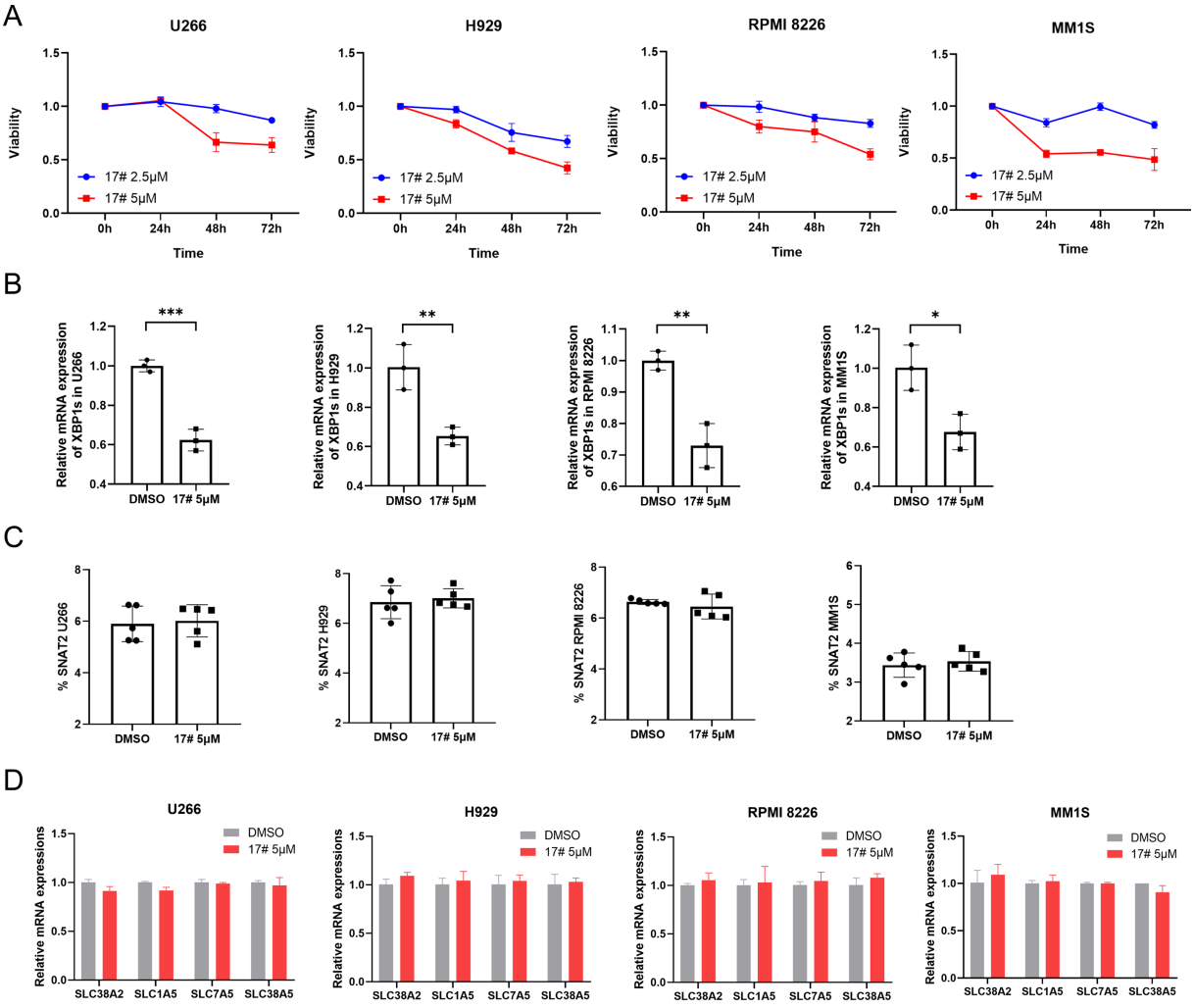

Figure 4 IRE1α inhibition suppresses the proliferation of MM cell lines independently of the XBP1-SLC38A2 axis. (A) MM cell lines were treated with 17# in complete medium. Viability of MM cell lines was assessed by CCK8. Data are presented as mean values±SD (n=3). (B) Relative mRNA expression of XBP1s in MM cell lines at 48 hours in (A) was detected by qRT-PCR. Data are presented as mean values±SD (n=3). Two-sided unpaired t-test, $^{*}p<0.05$, $^{**}p<0.01$, $^{***}p<0.001$. (C) Percentages of SNAT2 expressing MM cell lines at 48 hours in (A) were assessed by flow cytometry. Data are presented as mean values±SD (n=5). Two-sided unpaired t-test. (D) Relative mRNA expression of SLC38A2, SLC1A5, SLC7A5 and SLC38A5 in MM cell lines at 48 hours in (A) was detected by qRT-PCR. Data are presented as mean values±SD (n=3). Two-sided unpaired t-test. DMSO, dimethyl sulfoxide; MM, multiple myeloma; mRNA, messenger RNA; qRT-PCR, quantitative real-time polymerase chain reaction; SNAT2, sodium-coupled neutral amino acid transporter 2.

$CD8^+$ Tem/Teff cells was increased in BM cells from the 17# group (figure 5F). Further analysis showed that 17# treatment not only decreased the proportion of senescent $CD8^+$ T cells (figure 5G) but also enhanced the production of IFN-γ and perforin, which represented the effector cytokine and degranulation, respectively (figure 5H). In addition, 17# reduced the proportion of $B220^-CD138^+$ plasma cells and reversed the senescence of $CD8^+$ T cells in spleen samples (online supplemental figure 5A, B and C). Together, these results suggest that 17# treatment can effectively limit the growth of MM cells by protecting $CD8^+$ T cells against senescence, thereby potentiating their antitumor immune responses.

DISCUSSION

Our previous research demonstrated significantly elevated expression of the ER stress-related key transcription factor XBP1s in BM $CD8^+$ T cells from patients with MM. XBP1s directly repressed the expression of the glutamine transporter SLC38A2, resulting in impaired glutamine uptake and accelerated senescence of $CD8^+$ T cells. In this study, we examined the impact of IRE1α inhibition on $CD8^+$ T cells and found that compound 17# can reverse T-cell senescence and enhance antitumor responses by modulating mtROS levels. Our findings uncover a novel function of IRE1α inhibition in $CD8^+$ T cells, providing new strategies for targeting the immunological microenvironment in MM treatment.

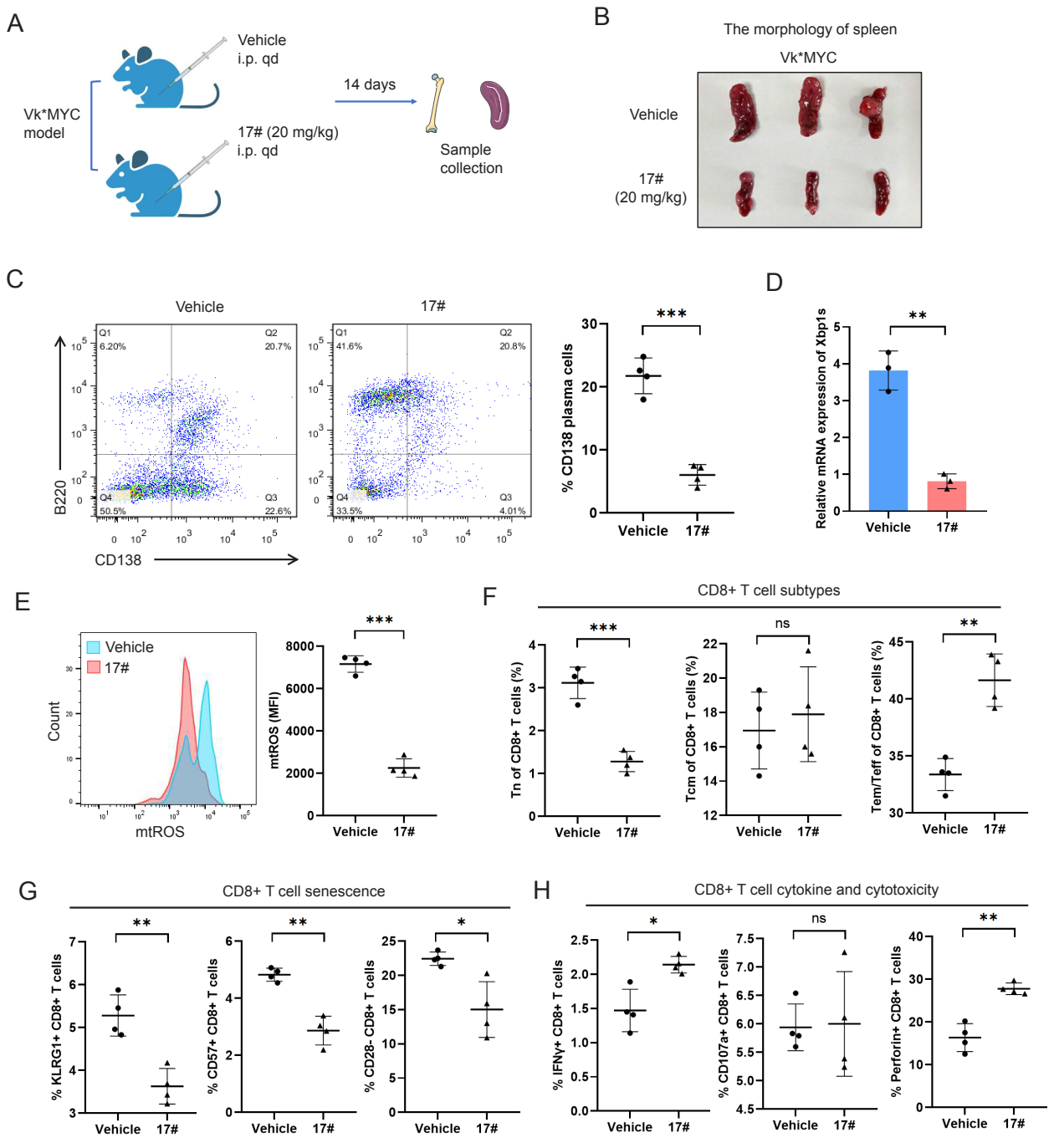

Figure 5 IRE1α inhibition reverses CD8$^+$ T-cell senescence and reduces tumor burden in Vk*MYC myeloma mouse model. (A) Work flow of in vivo experiments. The Vk*MYC mice were divided into two groups (n=5), which were, respectively, injected intraperitoneally with 17# (20 mg/kg) daily. After 14 days, the femoral BM samples and spleen samples were harvested. (B) The morphology of spleen obtained from Vk*MYC mice after treatment. (C) Percentages of B220$^-$CD138$^+$ expressing plasma cells from BM samples in Vk*MYC mice after treatment were assessed by flow cytometry. Data are presented as mean values±SD (n=4). Two-sided unpaired t-test, ***p<0.001. (D) Xbp1s mRNA levels of BM cells in Vk*MYC mice were detected by qRT-PCR. Data are presented as mean values±SD (n=3). Two-sided unpaired t-test, **p<0.01. (E) Mean fluorescence intensity of mtROS in BM CD8$^+$ T cells was assessed by flow cytometry. Data are presented as mean values±SD (n=4). Two-sided unpaired t-test, ***p<0.001. (F) Percentages of CD8$^+$ T-cell subsets from BM samples were assessed by flow cytometry. Data are presented as mean values±SD (n=4). Two-sided unpaired t-test, **p<0.01, ***p<0.001. (G, H) Percentages of senescence, cytokine, and cytotoxicity markers of BM CD8$^+$ T cells were assessed by flow cytometry. Data are presented as mean values±SD (n=4). Two-sided unpaired t-test, *p<0.05, **p<0.01. BM, bone marrow; IFN, interferon; i.p., intraperitoneal injection; MFI, mean fluorescence intensity; mRNA, messenger RNA; mtROS, mitochondrial reactive oxygen species; qRT-PCR, quantitative real-time polymerase chain reaction; Tcm, central memory T; Teff, effector T; Tem, effector memory T; Tn, naive T.

T-cell dysfunction, manifesting as either exhaustion or senescence, is a recurrent theme across diverse tumor microenvironments in various stages of cancer progression.[21 22] T-cell exhaustion, often induced by chronic infections and cancer, refers to a state in which effector T cells lose their normal functions.[23] Exhausted T cells are characterized by the upregulation of multiple inhibitory receptors, including PD-1, CTLA-4, CD160, TIM3, and LAG3.[24] Conversely, T-cell senescence is marked by a loss of normal proliferative capacity, which can be triggered by telomere-dependent and telomere-independent mechanisms.[25] Telomere-independent senescence can be induced by external factors such as cellular stress.[26] Meanwhile, T-cell senescence induced by the tumor microenvironment has also been identified as a state of T-cell dysfunction[27 28] and is characterized by mitochondrial dysfunction and the upregulated expression of CD57, KLRG1, along with the deficiency of costimulatory molecules such as CD27 and CD28.[25 29] Recent research by Professor Zemin Zhang's team has revealed that, compared with other types of cancer, MM shows no significant population of exhausted T cells,[30] suggesting that exhaustion may not be the primary type of T-cell resulting in immune suppression in MM. In our earlier work, senescence phenotypes were generally observed in cytotoxic T cells in patients with MM. However, the underlying mechanisms driving T-cell senescence in MM are not fully understand, and countering T-cell senescence may represent a pivotal checkpoint and effective strategy for anti-myeloma immunity.

To ameliorate the senescence of $CD8^+$ T cells in MM, we attempted to target the XBP1s-SLC38A2 axis using the IRE1α inhibitor 17#. We found that the IRE1α inhibitor can regulate mtROS levels. Mitochondria are the primary source of ROS, and mtROS, once viewed solely as a disruptor of cellular homeostasis leading to oxidative damage and accelerated aging, has now been recognized as a significant signaling molecule involved in senescence, inflammation, and cancer.[31] For mitochondria themselves, their replication and transcription processes require regulation by certain nuclear-encoded transcription factors. Among these, TFAM plays a major regulatory role, not only participating in the activation of mitochondrial transcription but also in the replication of the mitochondrial genome, stabilizing mitochondrial DNA, which is crucial for maintaining mitochondrial energy supply.[32] Studies have shown that in acute kidney injury, mtROS can disrupt TFAM-mediated mitochondrial DNA stability, leading to mitochondrial dysfunction.[33] Desdín-Micó *et al*[32] found that T cell-specific deletion of TFAM in mice can lead to immune senescence, causing premature aging in mice and triggering various age-related conditions. These results suggest that the upregulation of mtROS and low expression of TFAM are critical factors in T-cell senescence.

Our findings mechanistically connect IRE1α-XBP1s signaling to repression of the cGMP-PKG pathway, suggesting that pharmacological inhibition alleviates XBP1s-mediated transcriptional silencing of NPR2. NPR2, known as natriuretic peptide receptor 2, is the primary receptor for C-type natriuretic peptide (NPPC/CNP).[34] When CNP binds to NPR2, it activates particulate guanylate cyclase (pGC). The activated pGC catalyzes the conversion of GTP to cGMP, thereby increasing the intracellular levels of cGMP, which further activates its downstream target, cGMP-dependent protein kinase (PKG). PKG regulates various cellular functions by phosphorylating its target proteins. This is particularly significant given the established role of cGMP-PKG signaling in regulating mitochondrial fusion-fission dynamics,[20] which is a process essential for maintaining metabolic flexibility and stress resilience in T cells. Our data propose that 17# indirectly rescues mitochondrial dysfunction in senescent $CD8^+$ T cells by reactivating this pathway, potentially through enhanced mitochondrial membrane stabilization or mtROS buffering. Collectively, our findings position the NPR2-cGMP-PKG axis as an actionable node for reversing T-cell senescence in MM, with broader implications for immunotherapy in senescence-related malignancies.

The therapeutic potential of IRE1α inhibition presents actionable strategies for clinical translation. Synergy may be particularly evident with IMiDs like lenalidomide, where reversal of $CD8^+$ T-cell dysfunction could extend treatment durability, or with daratumumab, where enhanced antibody-dependent cell-mediated cytotoxicity (ADCC) efficacy might be achieved through reinvigorated cytotoxic T-cell activity. Translational success will likely depend on biomarker-driven patient stratification, including tumor-intrinsic markers (IRE1α/XBP1s overexpression) and microenvironmental features ($KLRG1^+CD57^+CD28^-$ senescent T-cell infiltration), potentially monitored via liquid biopsy.

The therapeutic specificity of IRE1α inhibition in myeloma is underpinned by the unique secretory biology of malignant plasma cells, which drives chronic ER stress and heightened reliance on IRE1α-XBP1s signaling compared with normal counterparts for maintaining protein homeostasis and proliferation.[35] This kind of dependence in turn makes MM cells more vulnerable to protein homeostasis disruption induced by IRE1α inhibitors. Meanwhile, tumor-infiltrating T cells face harsh microenvironmental conditions where moderate activation of UPR can mitigate adverse effects on T-cell survival. However, excessive or inappropriate UPR activation may lead to T-cell dysfunction. Our findings indicate that overactivation of the IRE1α-XBP1s pathway in $CD8^+$ T cells from patients with MM induces cellular senescence through impaired mitochondrial function. To maintain mitochondrial homeostasis, $CD8^+$ T cells appear to require relief from the suppression of SNAT2 and NPR2 mediated by IRE1α-XBP1s signaling.

While our study focuses on MM, the broader applicability of this strategy is supported by preliminary evidence in other ER stress-addicted hematologic malignancies. For instance, IRE1α inhibitors exhibit potent antitumor

effects in acute myeloid leukemia models and reverse chemoresistance in chronic myeloid leukemia and chronic lymphocytic leukemia by disrupting pro-survival XBP1s signaling.[36–38] Importantly, 17# exhibited selective activity in our assays, sparing non-malignant PBMCs and preserving effector functions of healthy donor-derived $CD8^+$ T cells. This selectivity may arise from two interrelated mechanisms: (1) the basal ER stress tolerance of normal cells, mediated by compensatory pathways such as PERK activation,[39] and (2) the metabolic fragility of senescent $CD8^+$ T cells in the myeloma microenvironment, which exhibit amplified mtROS susceptibility. These findings collectively suggest that therapeutic targeting of IRE1α may achieve a favorable risk-benefit profile in MM, with potential extension to other malignancies characterized by chronic ER stress adaptation.

In this study, we evaluated the effects of 17# on $CD8^+$ T cells and tumor cells using the Vk*MYC myeloma mouse model. The Vk*MYC model, driven by MYC transgenesis, accurately recapitulates the progressive transition from MGUS to smoldering MM and eventually active MM. It retains a complete immune system, making it suitable for investigating T-cell senescence mechanisms in MM pathogenesis and the effects of IRE1α inhibition on T-cell function.[40] A limitation of the Vk*MYC model is the potential development of B-cell-derived lymphoma or leukemia, which may result in splenomegaly. Notably, our analysis of clinical patient samples with MM revealed $CD8^+$ T-cell senescence phenotypes and upregulated UPR signaling. These findings were corroborated in the Vk*MYC mouse model, where treatment with an IRE1α inhibitor reversed T-cell senescence both in vitro and in vivo.

Correcting the immunosuppressive state of $CD8^+$ T cells in MM to restore their effective antitumor function is a critical area of focus in MM research. This project integrates cellular stress, glutamine metabolism, mitochondrial function, and immune senescence to investigate these interconnected processes. Our findings confirm that IRE1α inhibition not only reverses $CD8^+$ T-cell senescence and enhances anti-myeloma immune responses but also directly inhibits MM cell proliferation, achieving a "get-two-birds-with-one-stone" effect.

Author affiliations
[1]Department of Hematology, Ren Ji Hospital, Shanghai Jiao Tong University School of Medicine, Shanghai, China
[2]Shandong Provincial Key Laboratory of Precision Oncology, Shandong Cancer Hospital and Institute, Shandong First Medical University and Shandong Academy of Medical Sciences, Jinan, China
[3]The Chinese National Center for Drug Screening, Shanghai Institute of Materia Medica, Chinese Academy of Sciences, Shanghai, China

Acknowledgements We are indebted to all patients and donors who participated in this study.

Contributors JH designed the study. JH, HH, and YW recruited patients and obtained blood and bone marrow samples. YW designed and implemented a pipeline for sample processing and cell collection. YW, MC, and JuW performed bioinformatics analyses. YW and JiW designed and performed in vitro and in vivo experiments. FN synthesized and provided the IRE1α inhibitor. JH, ZL, and HH supervised the research. YW generated figures and drafted the manuscript. JH is the guarantor.

Funding This work was supported by the Shanghai Shenkang Hospital Development Center Funding (SHDC2020CR2070B), the National Natural Science Foundation of China (82400243, JJ Wang; 82370209, ZQ Liu) and the Collaborative Academic Innovation Project of Shandong Cancer Hospital (FC009).

Competing interests None declared.

Patient consent for publication Not applicable.

Ethics approval The study protocol was approved by the Ethics Committee of Ren Ji Hospital, Shanghai Jiao Tong University School of Medicine (approval #: 2019010), Shandong Cancer Hospital and Research Institute (approval#: SDTHEC2024006118). Participants gave informed consent to participate in the study before taking part.

Provenance and peer review Not commissioned; externally peer reviewed.

Data availability statement Data are available upon reasonable request. The data that support the findings of this study are available from the corresponding author upon request. The raw scRNA-seq data are deposited in the Genome Sequence Archive in National Genomics Data Center, Beijing Institute of Genomics (China National Center for Bioinformation), Chinese Academy of Sciences (http://ngdc.cncb.ac.cn/gsa-human), under Bioproject Accession HRA001600.

ORCID iD
Yike Wan http://orcid.org/0000-0003-1199-5755

REFERENCES

1 Kawano Y, Roccaro A, Azzi J, *et al*. Multiple Myeloma and the immune microenvironment. *CCDT* 2017;17:1.
2 Lomas OC, Tahri S, Ghobrial IM. The microenvironment in myeloma. *Curr Opin Oncol* 2020;32:170–5.
3 Yamamoto L, Amodio N, Gulla A, *et al*. Harnessing the Immune System Against Multiple Myeloma: Challenges and Opportunities. *Front Oncol* 2020;10:606368.
4 Kurachi M. CD8+ T cell exhaustion. *Semin Immunopathol* 2019;41:327–37.
5 Wan Y, Chen M, Li X, *et al*. Single-cell RNA sequencing reveals XBP1-SLC38A2 axis as a metabolic regulator in cytotoxic T lymphocytes in multiple myeloma. *Cancer Lett* 2023;562:216171.
6 Tungkum W, Jumnongprakhon P, Tocharus C, *et al*. Melatonin suppresses methamphetamine-triggered endoplasmic reticulum stress in C6 cells glioma cell lines. *J Toxicol Sci* 2017;42:63–71.
7 Dostálová A, Vlachová M, Gregorová J, *et al*. The endoplasmic reticulum and its signaling pathways - a novel target for multiple myeloma treatment. *Klin Onkol* 2023;36:440–6.
8 Papandreou I, Denko NC, Olson M, *et al*. Identification of an Ire1alpha endonuclease specific inhibitor with cytotoxic activity against human multiple myeloma. *Blood* 2011;117:1311–4.
9 Shao A, Xu Q, Spalek WT, *et al*. Development of Tumor-Targeting IRE-1 Inhibitors for B-cell Cancer Therapy. *Mol Cancer Ther* 2020;19:2432–44.
10 Rangel Rivera GO, Knochelmann HM, Dwyer CJ, *et al*. Fundamentals of T Cell Metabolism and Strategies to Enhance Cancer Immunotherapy. *Front Immunol* 2021;12:645242.
11 Zhang Y, Zhang Y, Sun K, *et al*. The SLC transporter in nutrient and metabolic sensing, regulation, and drug development. *J Mol Cell Biol* 2019;11:1–13.
12 Song W, Li D, Tao L, *et al*. Solute carrier transporters: the metabolic gatekeepers of immune cells. *Acta Pharm Sin B* 2020;10:61–78.

13 Wiley CD, Campisi J. The metabolic roots of senescence: mechanisms and opportunities for intervention. *Nat Metab* 2021;3:1290–301.
14 Kumar S, Paiva B, Anderson KC, *et al*. International Myeloma Working Group consensus criteria for response and minimal residual disease assessment in multiple myeloma. *Lancet Oncol* 2016;17:e328–46.
15 Huang H, Liu H, Liu C, *et al*. Disruption of the unfolded protein response (UPR) by lead compound selectively suppresses cancer cell growth. *Cancer Lett* 2015;360:257–68.
16 Li X, Chen M, Wan Y, *et al*. Single-cell transcriptome profiling reveals the key role of ZNF683 in natural killer cell exhaustion in multiple myeloma. *Clin Transl Med* 2022;12:e1065.
17 Subramanian A, Tamayo P, Mootha VK, *et al*. Gene set enrichment analysis: A knowledge-based approach for interpreting genome-wide expression profiles. *Proc Natl Acad Sci USA* 2005;102:15545–50.
18 Percie du Sert N, Hurst V, Ahluwalia A, *et al*. The ARRIVE guidelines 2.0: Updated guidelines for reporting animal research. *PLoS Biol* 2020;18:e3000410.
19 Chesi M, Matthews GM, Garbitt VM, *et al*. Drug response in a genetically engineered mouse model of multiple myeloma is predictive of clinical efficacy. *Blood* 2012;120:376–85.
20 Hildebrand S, Ibrahim M, Schlitzer A, *et al*. PDGF regulates guanylate cyclase expression and cGMP signaling in vascular smooth muscle. *Commun Biol* 2022;5:197.
21 Liu X, Si F, Bagley D, *et al*. Blockades of effector T cell senescence and exhaustion synergistically enhance antitumor immunity and immunotherapy. *J Immunother Cancer* 2022;10:e005020.
22 Thommen DS, Schumacher TN. T Cell Dysfunction in Cancer. *Cancer Cell* 2018;33:547–62.
23 Sen DR, Kaminski J, Barnitz RA, *et al*. The epigenetic landscape of T cell exhaustion. *Science* 2016;354:1165–9.
24 McLane LM, Abdel-Hakeem MS, Wherry EJ. CD8 T Cell Exhaustion During Chronic Viral Infection and Cancer. *Annu Rev Immunol* 2019;37:457–95.
25 Kasakovski D, Xu L, Li Y. T cell senescence and CAR-T cell exhaustion in hematological malignancies. *J Hematol Oncol* 2018;11:91.
26 Lanna A, Henson SM, Escors D, *et al*. The kinase p38 activated by the metabolic regulator AMPK and scaffold TAB1 drives the senescence of human T cells. *Nat Immunol* 2014;15:965–72.
27 Liu X, Hoft DF, Peng G. Senescent T cells within suppressive tumor microenvironments: emerging target for tumor immunotherapy. *J Clin Invest* 2020;130:133679:1073–83:.
28 Liu X, Hartman CL, Li L, *et al*. Reprogramming lipid metabolism prevents effector T cell senescence and enhances tumor immunotherapy. *Sci Transl Med* 2021;13.
29 Mittelbrunn M, Kroemer G. Hallmarks of T cell aging. *Nat Immunol* 2021;22:687–98.
30 Zheng L, Qin S, Si W, *et al*. Pan-cancer single-cell landscape of tumor-infiltrating T cells. *Science* 2021;374:abe6474.
31 Zhu D, Li X, Tian Y. Mitochondrial-to-nuclear communication in aging: an epigenetic perspective. *Trends Biochem Sci* 2022;47:645–59.
32 Desdín-Micó G, Soto-Heredero G, Aranda JF, *et al*. T cells with dysfunctional mitochondria induce multimorbidity and premature senescence. *Science* 2020;368:1371–6.
33 Zhao M, Wang Y, Li L, *et al*. Mitochondrial ROS promote mitochondrial dysfunction and inflammation in ischemic acute kidney injury by disrupting TFAM-mediated mtDNA maintenance. *Theranostics* 2021;11:1845–63.
34 Prickett TCR, Espiner EA, Pearson JF. Association of natriuretic peptides and receptor activity with cardio-metabolic health at middle age. *Sci Rep* 2024;14:9919.
35 Mimura N, Fulciniti M, Gorgun G, *et al*. Blockade of XBP1 splicing by inhibition of IRE1α is a promising therapeutic option in multiple myeloma. *Blood* 2012;119:5772–81.
36 Sun H, Lin D-C, Guo X, *et al*. Inhibition of IRE1α-driven pro-survival pathways is a promising therapeutic application in acute myeloid leukemia. *Oncotarget* 2016;7:18736–49.
37 Liu L, Zhao M, Jin X, *et al*. Adaptive endoplasmic reticulum stress signalling via IRE1α-XBP1 preserves self-renewal of haematopoietic and pre-leukaemic stem cells. *Nat Cell Biol* 2019;21:328–37.
38 Tang C-HA, Ranatunga S, Kriss CL, *et al*. Inhibition of ER stress-associated IRE-1/XBP-1 pathway reduces leukemic cell survival. *J Clin Invest* 2014;124:73448:2585–98:.
39 Hetz C, Zhang K, Kaufman RJ. Mechanisms, regulation and functions of the unfolded protein response. *Nat Rev Mol Cell Biol* 2020;21:421–38.
40 Wang J, Peng Z, Guo J, *et al*. CXCL10 Recruitment of γδ T Cells into the Hypoxic Bone Marrow Environment Leads to IL17 Expression and Multiple Myeloma Progression. *Cancer Immunol Res* 2023;11:1384–99.